ARTICLES

Mechanism of Collisional Heating in Electrospray Mass Spectrometry: Ion Trajectory Calculations

A. Hoxha,[†] C. Collette,[‡] E. De Pauw,[‡] and B. Leyh*[,†,§]

Laboratoire de Dynamique Moléculaire and Laboratoire de Spectrométrie de Masse, Département de Chimie, B6c, Université de Liège, Sart-Tilman, B-4000 Liège 1, Belgium

Received: July 19, 2000; In Final Form: May 21, 2001

To simulate the multicollisional heating process taking place in the intermediate pressure region of an electrospray source, ion trajectory calculations have been performed by introducing in the SIMION program a subroutine for handling the collision dynamics. The simulated internal energy distributions are compared with already available experimental distributions obtained by the "survival ion yield" method (Collette, C.; Drahos, L.; De Pauw, E.; Vékey, K. *Rapid Commun. Mass Spectrom.* **1998**, *12*, 1673). The latter have been satisfactorily reproduced by using a statistical model for the energy redistribution between the ion and the target gas. This model takes into account both activation and deactivation processes occurring upon collision in the acceleration/fragmentation region. It accounts for the important role of the number of degrees of freedom of the target on the shape of the internal energy distribution.

I. Introduction

Electrospray ionization (ESI) is a widespread ionization technique in mass spectrometry because of its capabilities for direct analysis of samples in solution, which are of great interest for the investigation of biological molecules. Moreover, the internal energy of the ions emitted from the electrospray source can be modulated, giving a great versatility to the method.[1] Electrospray mass spectrometry makes the study of weak interactions in solution possible as well as that of gas-phase fragmentations.[2−7] Controlled fragmentation can be induced indeed by the application of a voltage on electrostatic lenses located in the intermediate pressure region between the source and the mass analyzer.[1] The accelerated ions are then submitted to dissociating collisions (CID) with the ambient gas. By controlling the voltage applied in this region, it is possible to modulate the fragmentation yields of the ions. This activation technique has been used in the analysis of high mass polymers as well as in many other applications. Its main advantage is that it allows very fast CID scans that make multiple ion identification possible within the time frame of a chromatogram peak.

The influence of the accelerating voltage and the nature of the collision gas on the internal energy distributions of the ions produced by an electrospray source has been studied by De Pauw and co-workers.[8−10] Their electrospray source, which has been modeled in the present work, is that of a VG Platform mass spectrometer schematically represented in Figure 1. By investigating the dissociation of benzylpyridinium cations, these authors found that the two main parameters influencing the dissociation yields are the sampling cone potential difference with respect to the grounded skimmer cone (denoted by $V_{sampling}$ in Figure 1) and the nature of the collision gas. Increasing the sampling cone voltage and the mass of the collision gas induces a broadening and a shift of the internal energy distributions of the resulting ions toward higher energies, whereas the use of molecular targets leads to narrower distributions. A possible explanation of this behavior is the concomitant excitation of the internal degrees of freedom of the target, as observed in high energy collisions.[11]

It is noteworthy that the observed distributions are similar to Boltzmann distributions and have therefore tentatively been characterized by a unique "effective temperature" parameter. Furthermore, a linear relationship between the effective temperature and the accelerating voltage applied to the sampling cone, $V_{sampling}$, has been observed.[10]

The rationalization of these observations requires a better knowledge of the mechanisms of ion formation and collisional heating in the electrospray source. However, despite several fundamental studies,[6,7,12−14] the basic mechanisms of ESI are still poorly understood. The ion formation mechanism is still a controversial subject. On the other hand, because of their complexity, even the mechanisms involved in the in-source CID are not well understood and are very dependent on the experimental conditions. It is in fact difficult to model these processes because, in most commercial instruments, the experimental conditions are not strictly defined and hard to control. A few very interesting attempts in modeling have however been reported and are discussed in more detail now.

Hunt et al.[15] have modeled the motion of ions in the intermediate pressure region. Their model takes the gas dynamics of viscous air flow as well as the electric field focusing into account. They have shown that the ion motion between the

* To whom correspondence should be addressed.
[†] Laboratoire de Dynamique Moléculaire.
[‡] Laboratoire de Spectrométrie de Masse.
[§] Chercheur qualifié du F.N.R.S. (Belgium).

10.1021/jp002575o CCC: $20.00 © 2001 American Chemical Society
Published on Web 07/17/2001

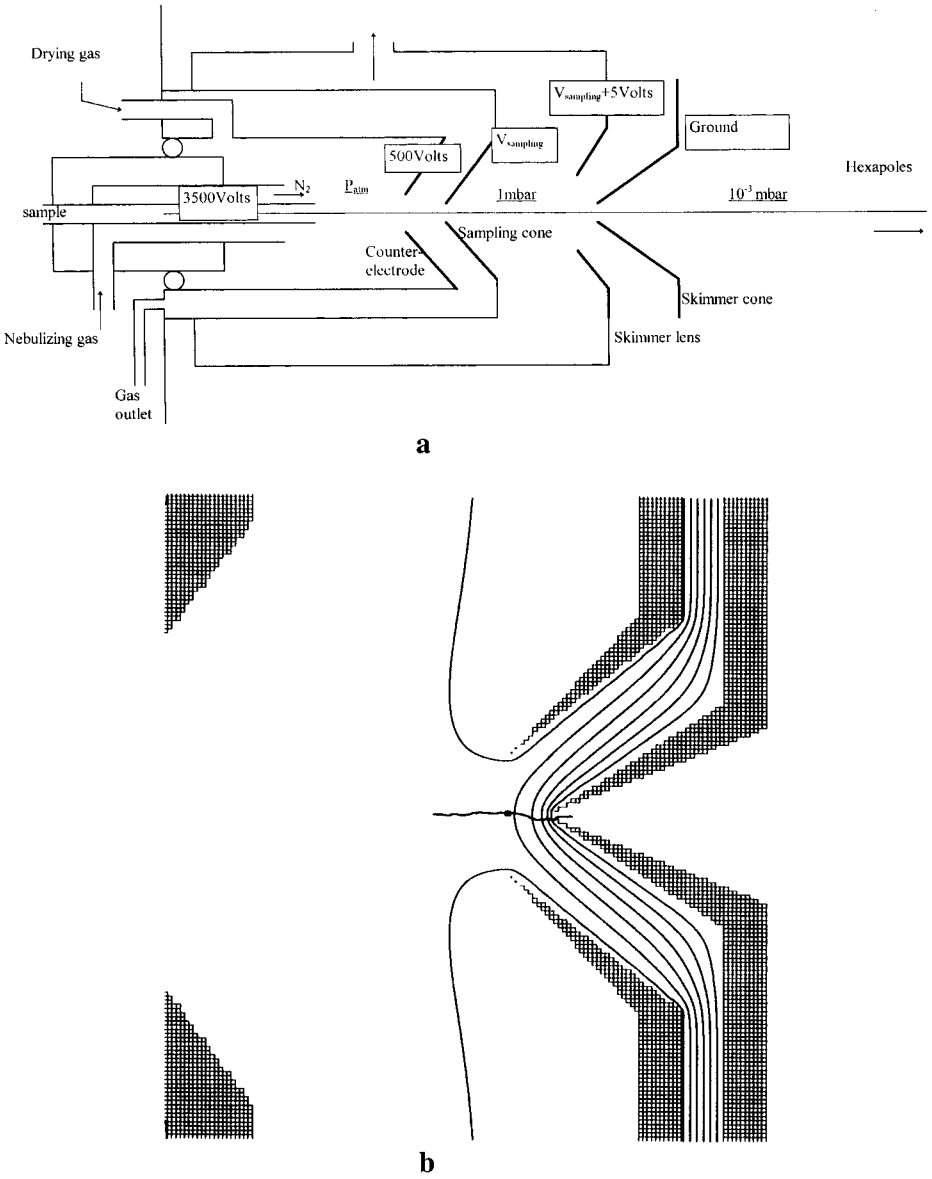

Figure 1. (a) Schematic representation of the electrospray source of the VG Platform instrument and (b) geometry of the relevant part of the source as simulated in SIMION, equipotential lines and one representative ion trajectory.

sampling cone and the skimmer cone can be described by two processes. Just after the sampling cone, the motion is controlled by the gas expansion. When the ions are near the skimmer cone, their motion is mainly controlled by the electric field induced by the potential on the sampling cone and the influence of the gas dynamics becomes negligible.

Recently, Schneider and Chen developed a semiquantitative model to predict the mean internal energy of electrosprayed ions.[16] Their model takes into account neither the influence of the source geometry on the acceleration of the ions nor the effect of desactivating collisions. They were nevertheless able to predict at which acceleration voltage the fragmentation onset takes place.

In the present work, we tried to get a better insight into the in-source collisional activation through ion trajectory simulations. The SIMION[17] ion optics program has been used to simulate the ion motion in the electric field. A subroutine has been written to include the collision dynamics and has been coupled to a statistical model for the energy transfer taking place at each collision event. Our goal is not to reach a perfect fit of the experimentally observed distributions but rather to gain a deeper understanding of the physics involved in the collisional activation region of the ESI source.

II. Experimental Conditions

As already mentioned, we have tried in this work to simulate, through ion trajectory calculations, the internal energy distributions of electrospray ions and we compared them to the experimental distributions obtained by De Pauw and coworkers.[8,9]

This work does not contain any new experimental data. We will nevertheless briefly discuss the experimental conditions in which the internal energy distributions presented here have been obtained[8,9] in order to help the reader to evaluate better the comparison between the experimental and the simulated data. The pressure gradient in the intermediate region of the electrospray source (Figure 1a), which is located between the atmospheric pressure source and the hexapoles (10^{-3} mbar), is maintained by the differential pumping in the hexapole region.

As a result, the pressure between the sampling cone and the skimmer cone decreases. Voyksner et al. propose that the mean free path of the ions in this region ranges between 10^{-8} and 10^{-4} m.[1] On the other hand, it has been experimentally demonstrated that the voltage applied to the sampling cone has a profound influence on the ion dissociation yield, whereas the electrospray voltage applied to the counter electrode does not affect the internal energy of the ions.[8] This is an important observation because it implies that, because of the very high number of collisions in the sampling cone region, ions arrive at the skimmer lens with almost no kinetic energy and their internal energy is built up in the acceleration region near the skimmer. The major contribution to the acceleration of the ions occurs close to the skimmer cone where the electric field is stronger. In that 2 mm long region, the mean free path is longer because of the lower pressure and the electric field to which the ions are submitted is stronger due to the tip effect of the skimmer.

III. Simulation Model for Collisional Heating

For the ion trajectory calculations, we used the SIMION[17] version 6.0 program. The motion of the ions in the electric field, i.e., the kinematics, is handled by SIMION, whereas a subroutine has been written in the SIMION programming language to treat the collision dynamics. Random collisions with target gas molecules, either at rest or characterized by an average thermal energy, are assumed. The projectile ion motion between two collisions is calculated by SIMION. The average distance between two successive collisions is governed in the SIMION subroutine by the mean free path, λ, introduced as a free parameter and allowed to vary within reasonable limits. At each collisional event, conservation of the center-of-mass energy and linear momentum has to be ensured. As the collisions are partially inelastic, the fraction of the relative kinetic energy which is converted into internal energy of the projectile had to be evaluated and injected into the SIMION subroutine. This essential point is treated in detail below. As a starting point for the trajectory simulations, we show in Figure 1b the relevant part of the modeled ion source with the corresponding equipotential lines. As a preview of the results, a representative projectile ion trajectory influenced by the multicollisional dynamics is also displayed.

Let us first consider a single collision event. Just before the collision, the ion possesses a kinetic energy in the laboratory frame KE_{lab} given by $m_{ion}v^2/2$. However, the kinematics of the collision is best analyzed in the center-of-mass frame to account for the conservation of linear momentum. During the collision, the kinetic energy of the center of mass, given by $KE_{CM} = m_{ion}/(m_{ion} + m_G)KE_{lab}$ where m_G is the mass of the target gas, is conserved. In the case of a completely inelastic collision, the relative kinetic energy $KE_{rel} = KE_{lab} - KE_{CM} = m_G/(m_{ion} + m_G)KE_{lab}$ is transformed into internal energy of the collision partners. In the general case, however, only a fraction, denoted by f, of this relative kinetic energy KE_{rel} is converted into internal energy of the ion. To estimate the value of f, a statistical model has been adopted, as we discuss now.

Let us assume that the interaction between the ion and the target lasts long enough to allow for the randomization of the total energy of the projectile + target system. This total energy is equal to the relative kinetic energy of the collision partners, KE_{rel}, plus the internal energy of the projectile ion and possibly the thermal energy of the target. When the projectile and the target separate after the collision, this total energy is partitioned between the dissociating partners as relative translational energy ϵ, as internal energy of the ion E_{int}, and as internal energy of the target gas E_G. In a purely statistical situation the probability of a given partitioning (E_{int}, E_G, and ϵ) at a total energy E_{total} is governed by the respective densities of states:

$$P(E_{int},E_G,\epsilon|E_{total}) = BN_{ion}(E_{int})N_G(E_G)N_\epsilon(\epsilon)\delta(\epsilon + E_G + E_{int} - E_{total}) \quad (1)$$

In this expression, the $N(E_i)$ are the densities of states for each particular kind of motion and B is a normalization constant. The δ function ensures the conservation of energy. Integrating over ϵ leads to:

$$P(E_{int},E_G|E_{total}) = BN_{ion}(E_{int})N_G(E_G)N_\epsilon(E_{total} - E_{int} - E_G) \quad (2)$$

Integration of this expression over all possible values of E_G gives the probability of obtaining an internal energy E_{int} of the projectile ion at a given total energy E_{total}.

$$P(E_{int}|E_{total}) = BN_{ion}(E_{int})\int_0^{E_{total} - E_{int}} N_G(E_G)N_\epsilon(E_{total} - E_{int} - E_G)\,dE_G \quad (3)$$

The translational density of states is simply $N_\epsilon(\epsilon) = C\epsilon^{1/2}$ with C being a normalization constant, whereas the classical expressions for the vibrational density of states lead to $N_{ion}(E_{int}) = C'(E_{int})^{s-1}$ and $N_G(E_G) = C''(E_G)^{p-1}$ where s and p are the number of vibrational degrees of freedom of the ion and of the target gas, respectively.[18,19] Introducing these expressions into eq 3 leads to

$$P(E_{int}|E_{total}) = B'(E_{int})^{s-1}\int_0^{E_{total} - E_{int}} (E_G)^{p-1}\sqrt{E_{total} - E_{int} - E_G}\,dE_G \quad (4)$$

with B' being a new constant including all normalization constants. The integral in eq 4 is known so that we finally obtain the following simple result:

$$P(E_{int}|E_{total}) = B''(E_{int})^{s-1}(E_{total} - E_{int})^{p+1/2} \quad (5)$$

It is clear that, for a given ion, the shape of this statistical distribution will strongly depend on the number of degrees of freedom of the target, p. Figure 2 displays the calculated statistical distributions for $p = 0$ and $p = 4$. From this figure, it can readily be seen that the distribution is broader for collisions involving target gases that possess a larger number of vibrational degrees of freedom. It must be noticed here that, by using the classical expressions for the densities of states, we assume in fact a perfect equipartition of the available energy between all degrees of freedom. This is certainly a poor approximation for the vibrations with the largest frequencies. The larger the frequency, the weaker will be the excitation of the corresponding mode. A simple way to handle this in a classical framework is to reduce artificially the number of vibrational degrees of freedom. It was assumed that only a fraction of 44% of the vibrational modes of the projectile participates in the energy randomization. This 0.44 factor is an empirical factor adopted by Franklin and Haney based on a comparison of statistical and experimental mean kinetic energy releases.[20]

The validity of this treatment has been checked by comparing the average relative translational energy release calculated using classical densities of states and using Klots' statistical treatment,[21,22] which takes the quantized nature of the vibrational

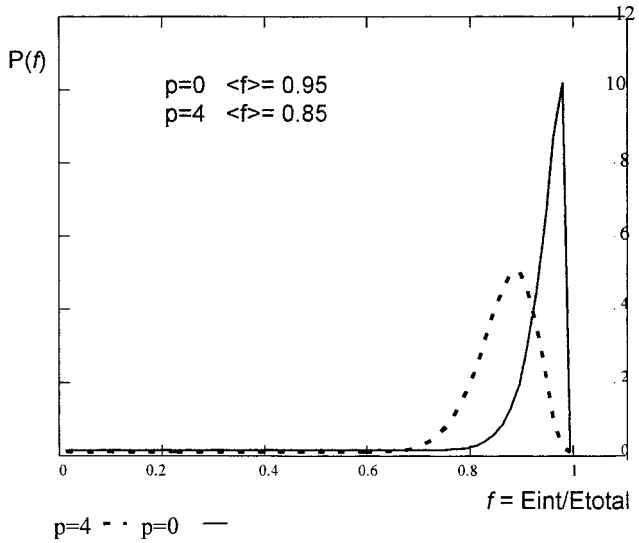

Figure 2. Probability of releasing, in a single collision, a fraction *f* of the total energy as internal energy of the ion. A typical value of *s* for a benzylpyridinium cation has been used in these calculations based on the statistical model described in the text ($s = 70 \times 0.44 = 31$).

TABLE 1: Mean Values of *f* Calculated Using Classical Densities of States and via Klots' Equation for Different Number of Vibrational Degrees of Freedom of the Target[a]

p	⟨*f*⟩ (classical densities of states)	⟨*f*⟩ (Klots)
0	0.95	0.93
1	0.93	0.88
2	0.89	0.85
3	0.87	0.81
4	0.85	0.79

[a] The projectile is assumed to be the *p*-chloro benzyl-pyridinium ion. The total energy is set at 3 eV.

motion into account. In this latter method, the individual vibrational frequencies are required and are taken as those of the *p*-chloro benzyl-pyridinium ion calculated at the B3LYP (6-31G) level within the Gaussian 94[23] package of programs. In the 2.8−3.4 eV internal energy range, it turned out that Klots results and the classical results were equivalent, provided an effective number of vibrational modes equal to 43−46% (or 36−55% in the 2−5.5 eV energy range) of the total number of modes was introduced in the classical treatment. This fraction is close to Haney and Franklin's empirical factor (44%).

It should be stressed again that Figure 2 represents the most statistical distribution of the internal energy of the ion obtained for a single collision. The SIMION program allows only the average ratio $f = \langle E_{\text{int}} \rangle / E$ to be introduced in the trajectory calculations. Mean values of the total energy fraction converted into internal energy of the ion are given in Table 1 as a function of the number of degrees of freedom of the target gas. The calculated value of *f* for a monatomic target gas is equal to 0.95 at a total energy of 3 eV. Notice that Table 1 gives for comparison both the value of *f* evaluated using classical densities of states with an effective number of degrees of freedom (44% of the total number) and using Klots' approach. Both *f* values are close. Bearing in mind that the size of the ion (in terms of degrees of freedom) is an influent parameter, these values compare favorably with the experimental value of $f = 0.92$ given by Futrell and al.[24] for collisions of benzene ions with Ar at 4.9 eV relative translational energy. At a total energy of 3 eV, i.e., close to the final energy reached in the activation process (see below), the value of *f* evaluated using Klots' theory[21,22] is equal to 0.93. The use of the empirical formulas of Drahos and Vekey[25] which do not need the prior knowledge of the vibrational frequencies leads in this case to a mean value of *f* equal to 0.915.

The above-described model for the energy transfer is based on a complete statistical redistribution of the energy available. In the absence of any precise information on the ratio between the collisional and the vibrational relaxation time scales, as well as on the propensity rules governing the energy transfer process in these systems, it is difficult to decide a priori to what extent the statistical assumption is valid. Our approach consists rather in considering the statistical limit as a guideline leading to a theoretical estimate of the energy distributions, which have then to be compared to the experimental data. As will be discussed in the next section, it has been necessary to introduce in certain cases a limited number of active vibrational modes of the target. This has an analogous effect as to adjust the value of *f* and corresponds to a restriction of the phase space visited by the collision partners. In this way, some flexibility is allowed with respect to a purely statistical situation.

IV. Results and Discussion

A. Internal Energy Distributions. Our goal is to model at best the sampling cone voltage and target gas influences on the internal energy distributions. The starting position of the ions was located on the spectrometer axis. It has been chosen to be the point where the ions first start feeling the attracting field of the skimmer (i.e., where the electrical field reverses from being repulsive because of the effect of the skimmer lens to being attractive because of the skimmer cone potential). Simulations have been run for populations of 1000 ions. In these simulations the mean free path of the ions was slightly scanned (between reasonable limits, i.e., between $10^{-5}-10^{-4}$ m) to best fit the experimental data. It soon became clear that, as pointed out by Voyksner,[1] the in-source CID is a slow heating process that includes not only activation but also deactivation processes during the collisions. Any realistic model has to take this effect into consideration. In our model, this is automatically taken into account because, at each collisional event *i*, the total energy of the projectile + target system, E^i_{total}, includes both the relative translational energy KE^i_{rel} and the internal energy of the ion impinging on the target, E^i_{int}. The internal energy of the ion prior to collision is therefore also statistically redistributed over all available degrees of freedom. During the course of our work, it was also realized that the thermal energy of the target gas, E_{therm}, must be considered in the total energy balance to reproduce the experimental results, especially when molecular targets with a large number of degrees of freedom are concerned. The total energy available for redistribution at collision *i* is then

$$E^{\,\text{i}}_{\text{total}} = KE^{\text{i}}_{\text{rel}} + E^{\text{i}}_{\text{int}} + E_{\text{therm}}$$

We are aware that this is only an average way of dealing with the thermal energy of the target. An appropriate way would be to consider the full velocity distribution of the target molecules as well as their internal energy distribution. However, as far as we are mainly concerned with the acceleration region where the projectile ions acquire relatively important velocities, the neglect of the individual target molecule velocities seems reasonable. Therefore, only the mean internal energy of the target has been considered. After collision *i*, the projectile ion will be left with an internal energy given by

$$E^{i+1}_{\text{int}} = fE^{\text{i}}_{\text{total}}$$

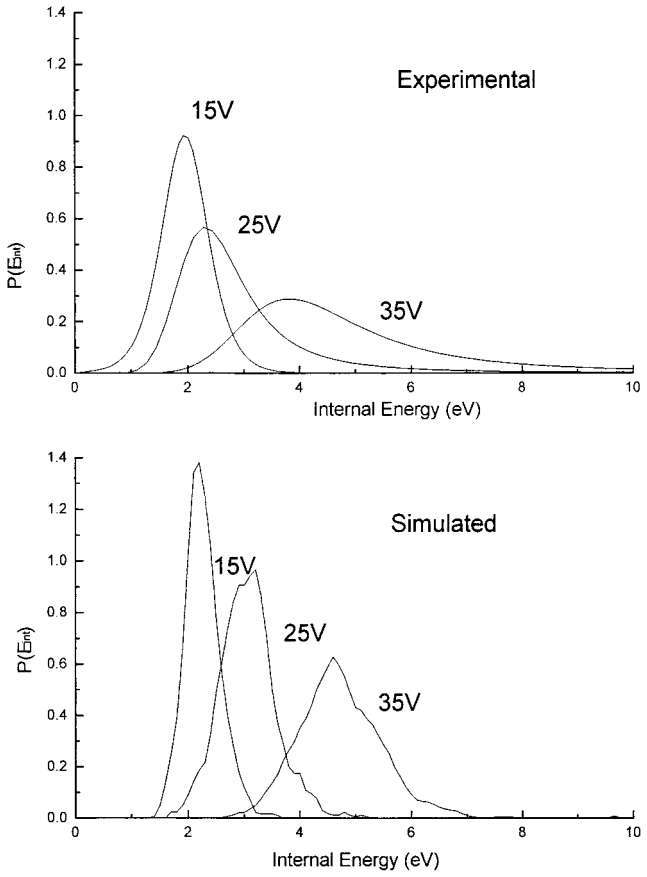

Figure 3. (a) Experimental (taken from refs 8 and 9) and (b) calculated (this work) internal energy distributions as a function of the cone voltage. The collision gas is N_2.

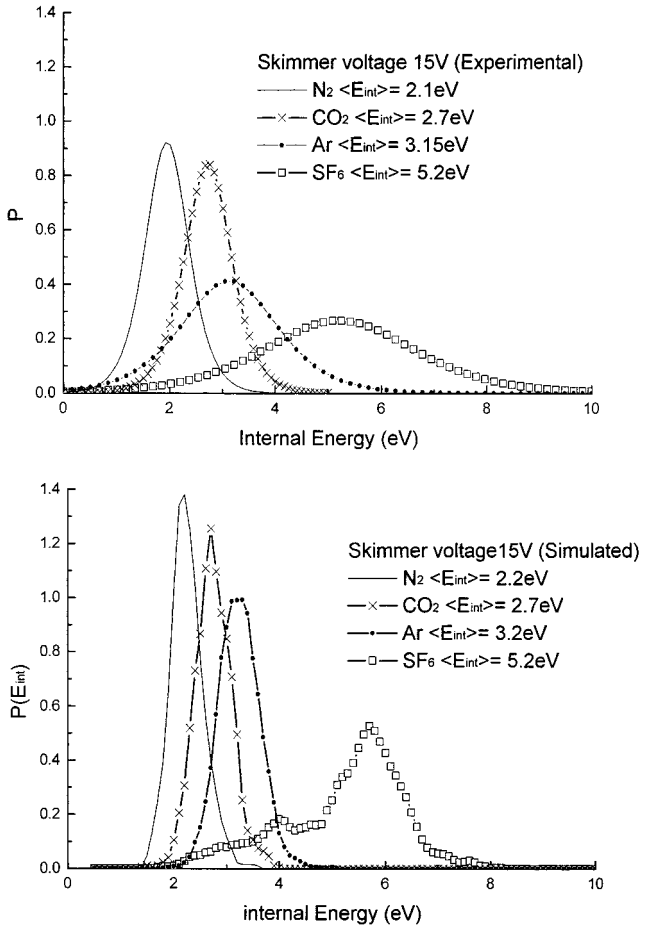

Figure 4. (a) Experimental (taken from refs 8 and 9) and (b) calculated (this work) internal energy distributions as a function of the collision gas. The cone voltage is set to 15 eV.

The thermal energy of an atomic gas is equal to $^3/_2kT$ per molecule, whereas for molecular gases, it has been calculated from experimental C_p values.[26] A nearly room temperature of 300 K has been used, in agreement with the assertion of Hunt et al.[15] that the collision gas thermalizes in the intermediate pressure region. With these improvements, we were able to reproduce the voltage dependence of the internal energy distributions. As can be seen in Figure 3, the calculated distributions for nitrogen as the collision gas at different sampling cone voltages are in good agreement with the experimental data of De Pauw and co-workers.[8,9] The mean free path used for these simulations is 4×10^{-5} m, a very reasonable value compared to those given by Voyksner et al.[1]. Figure 4 displays the calculated distributions for different collision gases at a given constant sampling cone voltage. Let us first concentrate on nitrogen, carbon dioxide, and argon. As illustrated in Figure 5, the mean values of the internal energy distributions are very sensitive to the value of the parameter f used, which is given in Table 2. Satisfactory agreement with the experimental data was reached by considering a unique active vibration for N_2, and only two of the four vibrational modes for CO_2.

The case of SF_6 is somewhat more problematic. To simulate the internal energy distribution displayed in Figure 4, four active vibrations have to be considered and a mean free path as large as 3×10^{-4} m was required. This could be rationalized by noting that the colliding gas has to expand through two orifices (the pepper pot and the skimmer lens) and that the expansion conditions are quite different for SF_6 with respect to the other gases. The large difference in ultimate number densities in the skimmer region is probably due to the difference in the γ parameter ($\gamma = C_p/C_v$) which governs the adiabatic expansion of a gas: γ is equal to $^5/_3$ for Ar, whereas it decreases to 1.095 for SF_6. As the γ parameter appears in the power of the expansion laws, a difference of nearly 1 order of magnitude in the ultimate pressures is not unreasonable.

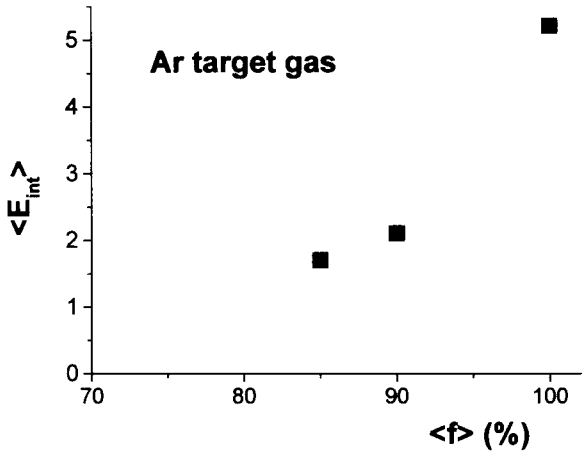

Figure 5. Influence of the fraction, f, of the total energy converted into internal energy at each individual collisional event, on the eventual average internal energy of a benzylpyridinium ion colliding with Ar.

TABLE 2: Values of f Used in the Simulations to Obtain the Distributions Displayed in Figure 4

collision gas	$\langle f \rangle$	collision gas	$\langle f \rangle$
Ar	0.95	CO_2	0.89
N_2	0.93	SF_6	0.85

A close comparison of Figures 3 and 4 reveals that although the experimental distributions[8,9] start to increase already at zero energy, the calculated ones show no contribution in that region. The presence of cold ions could be explained by the existence in the skimmer region of microdroplets which are cooled by evaporation. These relatively cold droplets release their ions very near the skimmer leaving them no time to accelerate and collisionally heat up. It must also be noticed that the experimental distributions are broader than the calculated ones. This can be at least partially explained by noting that our simple model neglects the spread of the initial conditions (spatial location and kinetic energy) for the ions: this spread will contribute to broaden the observed internal energy distribution. The multiple collision regime and the scattering of the initial conditions of the ions give rise to a broad statistical distribution. With these remarks in mind, it can be said that, in general, the agreement of the calculated internal energy distributions with the experimental ones is very satisfactory.

In the case of SF_6, however, the comparison is somewhat less favorable. In addition to the spread of the initial conditions, two arguments might be invoked to explain this situation. First, the amount of energy transferred at each collision is scattered over a distribution rather than being described by a single *f* parameter; this distribution will be broader in the case of SF_6 because of the larger number of degrees of freedom explaining partly the poorer agreement with experiment. Second, there is also a distribution of thermal energies of the target gas and not a single average value as postulated here, and this will contribute to further broaden the distribution.

We remind that our approach completely neglects the target gas flow dynamics in the intermediate pressure region. However, as showed by Hunt et al.,[15] the influence of the target gas flow on the motion of the ions is most important in the first expansion region and is more or less negligible in the CID region nearby the skimmer, where the strongly inhomogeneous electric field governs the projectile ion motion. Figure 6 illustrates how the internal energy deposition mainly takes place in a narrow region just before the skimmer. Only the progressive multicollisional activation of the ions has been simulated in this work. If an ion fragments, this will of course affect its trajectory, but this has not been included in our calculations which focused on the activation step. Our simulations show that the residence time of the ions in the acceleration/collision region where internal energy is built up is of the order of the microsecond. RRKM calculations by Collette et al.[9] on the benzylpyridinium ions show that an internal energy of about 4 eV has to be reached to fragment these ions in the microsecond time frame so that fragmentation before the skimmer is expected to be negligible but when SF_6 is used.

B. Effective Temperature Concept. The use of a single parameter for describing the internal energy distribution of the activated projectile ions and its interpretation as an "effective temperature" is a controversial subject. How could we understand the concept of an effective temperature in the case of electrospray?

In a system at thermal equilibrium, energy flows without constraints between all degrees of freedom, i.e., translational, rotational, and vibrational degrees of freedom. The vibrational, rotational, and translational energy distributions are all characterized by a single parameter: the temperature.

In the case of an electrospray source, a quasiequilibrium internal energy distribution is observed. However, it must be remembered that this distribution results from the energy flow between the relative translational motion and the internal modes.

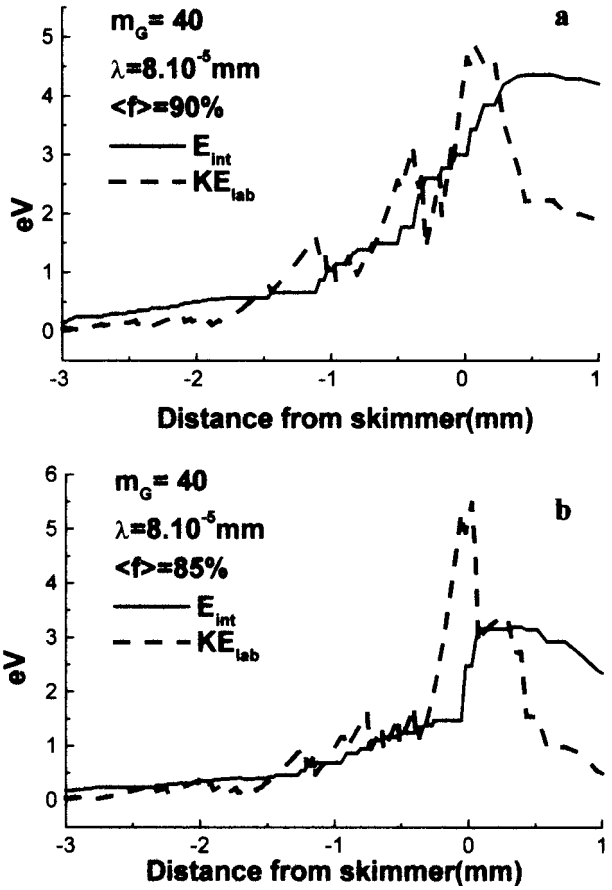

Figure 6. Internal energy and laboratory frame kinetic energy of benzylpyridinium ions colliding with a target of 40 amu, as calculated using the specified conditions. These data represent the outcome of a single trajectory run.

In the intermediate region of the electrospray source, the whole population of ions is submitted to a directed translational motion. Because of this motion and the collisions resulting from it, energy can be transferred to internal degrees of freedom. The number of collisions and the scattering of the initial conditions is such that a quasistatistical situation can be achieved. If we can assume that internal degrees of freedom are in thermal-like equilibrium with each other, it makes sense to postulate that they are also in quasiequilibrium with the translational motion that provides the energy.

With this in mind, we derived for each distribution of Figure 3b an effective temperature by assuming a perfect Boltzmann statistical behavior for either the average energy or its standard deviation. The result is displayed in Figure 7. The fact that both observables do not lead to the same effective temperature is an indication for the nonperfect Boltzmann behavior of the simulated distributions. This will be discussed later. An interesting observation is that a linear relationship between *T* and the sampling cone voltage appears. This is also observed experimentally and deserves some discussion.

We assume that we are dealing here with a population of ions which can more or less freely exchange energy between the relative translational motion and the internal degrees of freedom by means of collisions with a neutral gas. The energy exchange is different for every single ion, but as a whole the population behaves as if relative translation and the internal degrees of freedom were in thermal equilibrium and characterized by the **same** effective temperature parameter, T_{eff}.

$$T_{\text{eff, trans}} = T_{\text{eff, internal}} \tag{6}$$

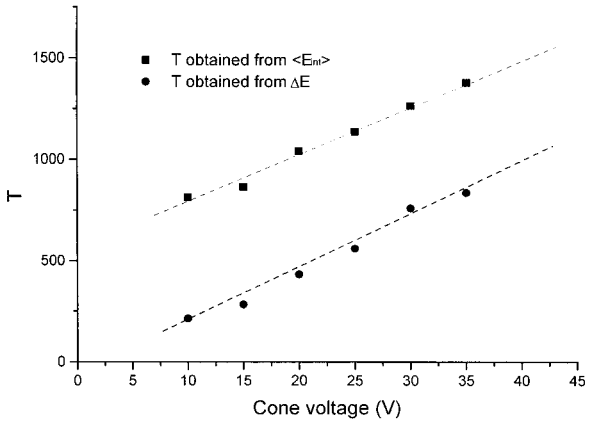

Figure 7. Temperature calculated from the average internal energies of the simulated distributions and from their standard deviations as a function of the acceleration voltage applied to the cone.

The translational energy of the ions in the laboratory frame is proportional to the accelerating voltage applied to the sampling cone:

$$KE_{\text{lab}} \propto zeV/l + bT_{\text{bath}} \tag{7}$$

where ze is the charge of the ion, V the cone voltage, l is the cone-skimmer distance, T_{bath} is the temperature of the bath gas, and b is a proportionality factor.

It must be noticed, however, that during the collisions only the relative translational energy

$$KE_{\text{rel}} = m_{\text{G}}/(m_{\text{G}} + m_{\text{ion}})KE_{\text{lab}} \tag{8}$$

is available for randomization. Because the average kinetic energy of a thermal gas is proportional to kT, we can write that

$$kT_{\text{eff, trans}} \propto m_{\text{G}}/(m_{\text{G}} + m_{\text{ion}})(zeV/l + bT_{\text{bath}}) \tag{9}$$

Combining (6) and (9) one gets

$$T_{\text{eff, internal}} \propto m_{\text{G}}/(m_{\text{G}} + m_{\text{ion}})V + b'T_{\text{bath}} \tag{10}$$

Of course, this does not mean necessarily that a given ion exchanges freely energy with other ions but that, as a whole and by means of a relatively important number of collisions with a neutral gas and starting from different initial conditions for many projectile ions, the system reaches eventually a quasithermal equilibrium state.

It seems therefore logical that the internal effective temperature calculated from the experimental distributions depends linearly on the accelerating voltage. Furthermore as also observed experimentally in the case of benzylpyridinium and leucine-enkephaline ions,[10] the temperature/voltage slope is proportional to the $m_{\text{G}}/m_{\text{ion}}$ mass ratio. If m_{ion} is much larger than m_{G}, then eq 10 shows that the effective temperature is inversely proportional to the ion mass, according to the experimental data.

The discrepancy between the effective temperature deduced from the average internal energy and from the standard deviations of the internal energy distributions is not unexpected because our distributions are found to reproduce well the average energies but underestimate the widths of the distributions leading to smaller effective temperatures based on the standard deviations. Possible explanations for this weakness have already been mentioned: neglect of the spread of the initial conditions, use of a single-valued energy transfer parameter f, and neglect of the thermal energy distribution of the target. Taking these effects into account would automatically broaden the distributions. However, the important point here is the linear relationship between the effective temperature and the skimmer voltage, which shows up with both numerical procedures.

V. Concluding Remarks

In this work, the internal energy distributions of collisionally activated ions in an electrospray source have been investigated by ion trajectory calculations. The internal energy of the ions is built up progressively during the multiple collisions close to the skimmer (within a distance of 2 mm, see Figure 6). In the adopted model, the available energy is supposed to be randomly redistributed between the projectile and the target at each collision event. Some flexibility can be allowed in the model by restricting the collision partners phase space to a subspace of active vibrations. By introducing this statistical model into ion trajectory calculations, the experimental internal energy distributions have been reasonably well reproduced. The present work accounts in a semiquantitative way for a number of experimental observations:

(i) The target mass dependence of the average energy reached by the heating process under the experimental conditions of De Pauw and co-workers[8−10] is reproduced. Schneider et al.,[27] however, showed very recently that, when working under expansion conditions that favor clustering of the collision gas, the degree of fragmentation as a function of the collision gas mass can be reversed, i.e., a lighter gas such as N_2 brings about a more extensive fragmentation than an heavier one like Ar or Kr.

(ii) The average internal energy depends also on the number of vibrational degrees of freedom of the target.

(iii) The thermal energy of molecular targets represents a nonnegligible contribution to the average energy transferred to the projectile; this is also in favor of a statistical image of the energy transfer.

(iv) The effective temperature concept can be substantiated as well as its dependence on the sampling cone voltage and on the projectile mass.

An important result which emerges also from the present work is the influence of the strong inhomogeneity of the electric field resulting from the cone voltage. Only in a very limited part (≈2 mm) of the intermediate pressure region, i.e., very close to the skimmer, are the ions subjected to a strong acceleration. Nearly 90% of the internal energy uptake takes place in this narrow region (Figure 6).

Yet another valuable information that can be extracted from the trajectory calculations is an estimate of the residence time of the ions in the acceleration/collision region. It has been calculated in this work to be of the order of the microsecond. Dissociations faster than the microsecond can occur inside the electrospray source.

We believe that although the present approach is far from being perfect it contains the main physics involved in the collisional heating process. Further refinements are of course possible, such as including the gas flow dynamics into trajectory calculations. On the other hand, confrontation of our model to new experimental results and other instruments would be extremely useful.

Acknowledgment. The authors thank Dr. G. Dive for the ab initio calculation of the vibrational frequencies of the benzylpyridinium ions and Dr. K. Vekey for very interesting discussions. We are grateful to the University of Liège for financial

support. This work has also been supported by the "Actions de Recherche Concertée (ARC)" (Direction de la Recherche Scientifique—Communauté Française de Belgique). B.L. is indebted to the F.N.R.S. (Belgium) for a research associate position.

References and Notes

(1) Voyksner, R. D.; Pack, T. *Rapid Commun. Mass Spectrom.* **1991**, *5*, 263.
(2) Fenn, J. B.; Mann, M.; Meng, C. K.; Wong, S. F.; Whitehouse, C. M. *Mass Spectrom. Rev.* **1990**, *9*, 37.
(3) Ganem, B.; Li, Y.-T.; Henion, J. D. *J. Am. Chem. Soc.* **1991**, *113*, 6294.
(4) Hopfgartner, G.; Piguet, C.; Henion, J. D.; Williams, A. F. *Helv. Chim. Acta* **1993**, *76*, 1759.
(5) Przybylski, M.; Glocker, M. O. *Angew. Chem.* **1996**, *35*, 806.
(6) Smith, R. D.; Loo, J. A.; Barinaga, C. J.; Edmonds, C. G.; Udseth, H. R. *J. Am. Soc. Mass Spectrom.* **1990**, *1*, 53.
(7) Smith, R. D.; Light-Wahl, K. J. *Biol. Mass Spectrom.* **1993**, *22*, 493.
(8) Collette, C.; De Pauw, E. *Rapid Commun. Mass Spectrom.* **1998**, *12*, 165.
(9) Collette, C.; Drahos, L.; De Pauw, E.; Vékey, K. *Rapid Commun. Mass Spectrom.* **1998**, *12*, 1673.
(10) Drahos, L.; Heeren, R. M. A.; Collette, C.; De Pauw, E.; Vékey, K. *J. Mass Spectrom.* **1999**, *34*, 1373.
(11) Leyh, B.; Hoxha, A. *Chem. Phys.* **1994**, *179*, 583.
(12) Fenn, J. B.; Mann, M.; Meng, C. K.; Wong, S. F.; Whitehouse, C. M. *Science* **1989**, *246*, 64.
(13) Fenn, J. B. *J. Am. Soc. Mass Spectrom.* **1993**, *4*, 524.
(14) Fenn, J. B.; Rosell, J.; Meng, C. K. *J. Am. Soc. Mass Spectrom.* **1997**, *8*, 1147.
(15) Hunt, S. M.; Sheil, M. M.; Belov, M.; Derrick, P. J. *Anal. Chem.* **1998**, *70*, 1812.
(16) Schneider, B. B.; Chen, D. D. Y. *Anal. Chem.* **2000**, *72*, 791.
(17) Dahl, D. SIMION 3D *43rd ASMS Conference on mass spectrometry and allied topics*, May 21−26; Atlanta, Georgia, 1995; p 717.
(18) Baer, T.; Hase, W. L. *Unimolecular Reaction Dynamics. Theory and Experiments*; Oxford University Press: New York, 1996.
(19) Tolman, R. C. *The Principles of Statistical Mechanics*; Oxford University Press: London, 1938.
(20) Haney, M. A.; Franklin, J. L. *J. Chem. Phys* **1968**, *48*, 4093.
(21) Klots, C. E. *J. Phys. Chem.* **1971**, *75*, 1526.
(22) Klots, C. E. *J. Chem. Phys.* **1973**, *58*, 5364.
(23) Frisch, M. J.; Trucks, G. W.; Schlegel, H. B.; Gill, P. M. W.; Johnson, B. G.; Robb, M. A.; Cheeseman, J. R.; Keith, T. A.; Petersson, G. A.; Montgomery, J. A.; Raghavachari, K.; Al-Laham, M. A.; Zakrzewski, V. G.; Ortiz, J. V.; Foresman, J. B.; Cioslowski, J.; Stefanov, B. B.; Nanayakkara, A.; Challacombe, M.; Peng, C. Y.; Ayala, P. Y.; Chen, W.; Wong, M. W.; Andres, J. L.; Replogle, E. S.; Gomperts, R.; Martin, R. L.; Fox, D. J.; Binkley, J. S.; Defrees, D. J.; Baker, J.; Stewart, J. P.; Head-Gordon, M.; Gonzalez, C.; Pople, J. A. *Gaussian 94*, revision D.4; Gaussian, Inc.: Pittsburgh, PA, 1996.
(24) Chawla, R.; Shukla, A.; Futrell, J. H. *Int. J. Mass Spec. Ion Proc.* **1997**, *165/166*, 237.
(25) Drahos, L.; Vekey, K. *J. Am. Soc. Mass Spectrom.* **1999**, *10*, 323.
(26) NIST Chemistry Webbook at URL *http://webbook.nist.gov/chemistry/*.
(27) Schneider, B. B.; Douglas, D. J.; Chen, D. D. Y. *Rapid Commun. Mass Spectrom.* **2001**, *15*, 249.